Rock and Soil Mechanics

Volume 44 | Issue 5 Article 9

8-21-2023

Analysis of lateral bearing capacity of flexible single pile under vertical-horizontal loading path in sand foundation

Jie JIANG
Key Laboratory of Disaster Prevention and Structural Safety of Ministry of Education, Guangxi University, Nanning, Guangxi 530004, China, School of Civil Engineering and Architecture, Guangxi University, Nanning, Guangxi 530004, China, Guangxi Key Laboratory of Disaster Prevention and Engineering Safety, Guangxi University, Nanning, Guangxi 530004, China

Chen-zhi FU
School of Civil Engineering and Architecture, Guangxi University, Nanning, Guangxi 530004, China

Wen-cheng CHAI
School of Civil Engineering and Architecture, Guangxi University, Nanning, Guangxi 530004, China

Xiao-duo OU
Key Laboratory of Disaster Prevention and Structural Safety of Ministry of Education, Guangxi University, Nanning, Guangxi 530004, China, School of Civil Engineering and Architecture, Guangxi University, Nanning, Guangxi 530004, China, Guangxi Key Laboratory of Disaster Prevention and Engineering Safety, Guangxi University, Nanning, Guangxi 530004, China

Recommended Citation

JIANG, Jie; FU, Chen-zhi; CHAI, Wen-cheng; and OU, Xiao-duo (2023) "Analysis of lateral bearing capacity of flexible single pile under vertical-horizontal loading path in sand foundation," *Rock and Soil Mechanics*: Vol. 44: Iss. 5, Article 9.
DOI: 10.16285/j.rsm.2022.5885
Available at: https://rocksoilmech.researchcommons.org/journal/vol44/iss5/9

Rock and Soil Mechanics 2023 44(5): 1375−1384 ISSN 1000−7598
https: //doi.org/10.16285/j.rsm.2022.5885 http://rocksoilmech.researchcommons.org/journal

Analysis of lateral bearing capacity of flexible single pile under vertical-horizontal loading path in sand foundation

JIANG Jie[1, 2, 3], FU Chen-zhi[2], CHAI Wen-cheng[2], OU Xiao-duo[1, 2, 3]

1. Key Laboratory of Disaster Prevention and Structural Safety of Ministry of Education, Guangxi University, Nanning, Guangxi 530004, China
2. School of Civil Engineering and Architecture, Guangxi University, Nanning, Guangxi 530004, China
3. Guangxi Key Laboratory of Disaster Prevention and Engineering Safety, Guangxi University, Nanning, Guangxi 530004, China

Abstract: There are few theoretical studies on lateral bearing capacity of flexible single pile under vertical-horizontal loading path in sand foundation and the influence of pre-applied vertical load on *p*-*y* curve is rarely considered. In view of this, the ultimate soil resistance of hyperbolic *p*-*y* curve was modified accounting for compacting effect of the sandy soil around the pile under the vertical force applied in advance. Cosine function was used to characterize the distribution of radial earth pressure on the passive side. The relationship between the maximum radial earth pressure on the passive side and the total soil resistance was proposed, and the analytical expression of the shaft resisting moment on the passive side was derived. Taking an included angle β between the direction of friction resistance and the vertical direction into account, the variation of pile axial force induced by friction resistance was corrected and its computational formula was obtained. The differential equation of pile deflection was established considering the modified *p*-*y* curve, the variation of axial force caused by pile dead weight and friction resistance, the *P*-Δ effect and the shaft resisting moment. The numerical solution was obtained by MATLAB program. The correctness of the proposed method was verified by comparing the calculated results with the existing simulations and measurements. On this basis, the influence of vertical force applied in advance on lateral bearing capacity of single pile was discussed. The results show that the computational formula of the variation of pile axial force deduced in this paper can more accurately describe the influence of friction resistance on pile axial force and can be used for large deformation conditions. The vertical force applied in advance can enhance the lateral bearing capacity of flexible single pile. The enhancement gradually decreases with the increase of the vertical force applied in advance.

Keywords: sand foundation; flexible single pile; vertical-horizontal loading path; lateral bearing capacity; numerical solution

1 Introduction

The pile foundations of offshore wind farms and bridges are first subjected to the vertical loads caused by the dead weight of the structure, and subsequently to the lateral loads generated by wind, water scouring, and earthquakes[1−5]. The interaction between the vertical and lateral loads has not been considered in the conventional methods; the two are considered separately, and the pile displacement and the internal force are calculated according to the superposition principle. This method is only applicable to cases where the elastic deformation is small, with certain limitations[6]. However, the response of pile under pre-applied vertical loads and then followed by lateral loads is significantly different from that under pure lateral load [7]. The effect of pre-applied vertical loads on the lateral response needs to be accounted for in optimal design although the lateral bearing capacity of flexible single pile is a key in design. Therefore, it is necessary to further study the calculation of the lateral bearing capacity under pre-applied vertical loads.

Abbas et al.[7], Lu et al. [8], and Zhao et al.[9] conducted model tests to study the lateral bearing characteristics of single pile under the $V\rightarrow H$ (V for vertical force, H for horizonal force) loading path. They found that the pre-applied vertical loading could increase the lateral stiffness of the surrounding soils and reduce the lateral displacement the pile. The same conclusions were obtained using the three-dimensional finite element method by Zou et al. [10] and Karthigeyan et al. [11]. To discuss the effect of slenderness ratio, Farhan et al.[12] studied the lateral bearing capacity of single pile with pre-applied vertical loads at different slenderness ratios through model tests, and the results showed that the effect of pre-applied vertical loads on the lateral bearing capacity decreased with the increase of slenderness ratio. The key to the theoretical analysis of laterally loaded pile is how to determine the *p*–*y* (*p* for soil resistance, *y* for pile lateral displacement) curve, but none of the above studies have discussed how the pre-applied vertical load affects the parameters related to the *p*–*y* curve, which restricts the development of theoretical approaches. In view of this, Mu et al.[13] plotted the *p*–*y* curves under different pre-applied vertical forces through a series of model tests and proposed a modified empirical formula for the ultimate soil resistance under different pre-applied vertical forces, which provided an idea for the subsequent theoretical analysis.

In summary, the studies on the lateral bearing characteristics of single pile under the $V\rightarrow H$ loading path have mainly focused on model testing and numerical simulations, with few theoretical analysis.

Received: 13 June 2022 Accepted: 28 September 2022
This work was supported by the National Natural Science Foundation of China (52068004), the Interdisciplinary Scientific Research Foundation of Guangxi University (2022JCB012) and the Key Research Projects of Guangxi (AB19245018).
First author: JIANG Jie, male, born in 1979, Postdoctoral research fellow, Professor, majoring in theoretical and applied research on pile foundation engineering. E-mail: jie_jiang001@126.com

Chatterjee et al. [14] provided an elastic solution for the lateral bearing capacity of single pile under the pre-applied vertical load, accounting for the second order effect (i.e. $P-\Delta$ effect, P for pile axial force, Δ for pile lateral displacement) with only the disadvantage of the $P-\Delta$ effects but without the effect of the pre-applied vertical load on the parameters related to the *p*–*y* curve considered, i.e. the benefit of the pre-applied vertical load on the lateral bearing capacity was ignored, which cannot accurately reflect the effect of the pre-applied vertical load on the lateral bearing capacity.

Following these ideas, the ultimate soil resistance of the hyperbolic *p*–*y* curve was modified by considering the pre-applied vertical force, the cosine function was used to characterize the radial earth pressure distribution on the passive side, and thus the relationship between the maximum radial earth pressure on the passive side and the total soil resistance was proposed. On this basis, the analytical expressions for the shaft resisting moment on the passive side and for the variation of pile axial force considering the angle β between the direction of frictional resistance and the vertical direction were derived. The differential equation of pile deflection was established accounting for the modified *p*–*y* curve, the variation of pile axial force caused by pile dead weight and frictional resistance on the passive side, the $P-\Delta$ effect, and the shaft resisting moment. The numerical solution was obtained by MATLAB and then compared with the existing measurements to verify the proposed method and to discuss the effect of the pre-applied vertical force on the lateral bearing capacity of flexible single pile, which can be used for engineering reference.

2 Computational model

2.1 Basic assumptions

For sand foundations, the effect of pre-applied vertical forces on the lateral bearing capacity of single pile is mainly in three aspects:

(1) The pre-applied vertical force causes the compacting effect on the soil around the pile, thus increasing the ultimate soil resistance.

(2) The pre-applied vertical force generates the $P-\Delta$ effect which becomes more obvious as the lateral displacement increases.

(3) The vertical frictional resistance exists on the pile, which induces variation of the pile axial force along the depth and creates the shaft resisting moment.

Therefore, the new equilibrium differential equation can be established by modifying the ultimate soil resistance and considering the $P-\Delta$ effect, the variation of axial force, and the shaft resisting moment, to set up the computational model of the lateral bearing capacity of flexible single pile under the $V\rightarrow H$ loading path. The following assumptions have been made for the convenience of calculation:

(1) The pile material is isotropic and homogeneous. The cross-section area and flexural stiffness always remains constant.

(2) The friction coefficient of the pile–soil interface does not vary with depth.

(3) The soil on the active side is detached from the pile. Only the vertical frictional resistance on the passive side is considered.

2.2 Soil resistance

O'Neill et al. [15] systematically evaluated the *p*–*y* curves of pile foundations in sand, compared various forms of *p*–*y* curves through a series of lateral loading tests, and believed that the hyperbolic method was the most accurate and easy to use. The hyperbolic *p*–*y* model is shown in Fig. 1. Therefore, the hyperbolic *p*–*y* model was employed in this paper to describe the non-linear relationship between the lateral soil resistance and the lateral displacement, with the following expression:

$$p=\frac{y}{1/k_{\mathrm{h,ini}}+y/p_{\mathrm{u}}} \tag{1}$$

where: $k_{\mathrm{h,ini}}$ is the initial subgrade reaction modulus, $k_{\mathrm{h,ini}}=n_{\mathrm{h,max}}z$; z is the depth; $n_{\mathrm{h,max}}$ is the coefficient of modulus of initial subgrade reaction, which can be determined from the table in literature [16]; and p_{u} is the ultimate soil resistance.

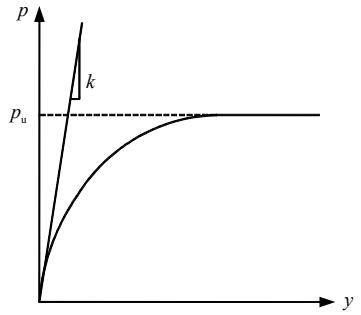

Fig. 1 Hyperbola *p*–*y* model

The ultimate soil resistance is increased, considering the compacting effect of the pre-applied vertical force on the soil around the pile. The compacting effect at different depths is related to the vertical frictional resistance at the pile–soil interface. The compacting degree gradually increases from 0 to the maximum as the vertical frictional resistance increases from 0 to the limit value. To date, few studies have been conducted and no computational model has been proposed to characterize the relationship between the ultimate soil resistance and the vertical frictional resistance at the pile–soil interface. In addition, the vertical frictional resistance varies non-linearly along the depth and is related to the vertical force at the pile top, which makes the issue more complex. Mu et al. [13] plotted the *p*–*y* curves at different depths under different vertical forces and developed an empirical formula for the ultimate soil resistance which is only related to the vertical force as simplification. The empirical formula is adopted to quantify the compacting effect of the pre-applied vertical force on the soil around the pile, i.e., the vertical force and the ultimate soil resistance are used for quantification. The larger the vertical

force, the greater the friction at the pile–soil interface, the greater the compacting effect, and the greater the ultimate soil resistance. The computational formula is as follows:

$$p_{\mathrm{u}}=\left(1+3\frac{V}{V_{\mathrm{ult}}}\right)p_{\mathrm{u0}} \tag{2}$$

where V is the vertical force at the pile top; V_{ult} is the vertical ultimate bearing capacity; p_{u0} is the ultimate soil resistance under pure lateral load. For pile foundations in sand subjected to pure lateral load, the ultimate soil resistance around the pile can be considered to increase linearly along the depth. Zhu et al.[17] suggested taking $p_{\mathrm{u0}}=\xi K_{\mathrm{p}}\gamma z d$, K_{p} being the coefficient of passive earth pressure, and $K_{\mathrm{p}}=\tan^2(45^\circ+\varphi/2)$; φ is the internal friction angle; γ is the unit weight of soil; and ξ is the coefficient of ultimate soil resistance, with a value range of 3–9.

2.3 Axial force and shaft resisting moment

For piles subjected to active loads, the soil on the active side and the pile trend to detach from each other, and the radial earth pressure on the passive side is much greater than the one on the active side which is assumed to be zero in the calculation and only the passive side radial earth pressure is considered [18–19]. The vertical frictional resistance on the passive side can cause changes in the pile axial force and generate a shaft resisting moment on the pile section, which both affect the lateral bearing capacity of the pile. The axial force variation and the shaft resisting moment can be solved according to the radial earth pressure on the passive side, so the key is how to accurately determine the radial earth pressure on the passive side. The significant deviation of the calculated radial earth pressure on the passive side from the actual one can cause the deviation of the calculated pile axial force variation and shaft resisting moment, thus leading to overestimating (or underestimating) the lateral bearing capacity.

When the lateral displacement occurs, the pile compresses the soil on the passive side, causing changes in the radial earth pressure at various points on the passive side. The compression is closely related to the lateral displacement. Therefore, the radial earth pressure on the passive side can be determined from two aspects—its distribution around the pile and its variation with the lateral displacement.

The previous studies [20–23] show that the radial earth pressure on the passive side is non-uniformly distributed, as shown in Fig.2. Zhang et al.[18] obtained the radial earth pressure on the passive side based on the cavity expansion theory, but the solution of this method is complicated and not easy for application. For the simplicity, the cosine function is adopted to characterize the distribution of the radial earth pressure. The relationship between the radial earth pressure at a point on the passive side $\sigma_{\mathrm{pr,i}}$ and the maximum radial earth pressure $\sigma_{\mathrm{pr,max}}$ can be expressed as

$$\sigma_{\mathrm{pr,i}}=\sigma_{\mathrm{pr,max}}\cos\theta \tag{3}$$

where θ is the angle between the radius of some point on the passive side and the pile lateral displacement.

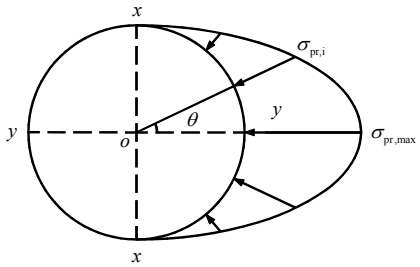

Fig. 2 Distribution of radial earth pressure on passive side

The following two examples were used to verify the applicability of Eq. (3) throughout the process of a laterally loaded pile reaching the ultimate bearing capacity. Prasad et al.[20] studied the ultimate bearing capacity of laterally loaded single pile by means of model tests and measured the distribution of earth pressure on the passive side. The test determined the distribution under the condition of a relative density of 0.75 and an ultimate bearing capacity of 1 790 N. The radial earth pressure at various points on the passive side was calculated by using Eq.(3) based on the maximum radial earth pressure (earth pressure at $\theta=0°$) and then compared with the measured results, as shown in Fig.3. The distribution of the radial earth pressure on the passive side is non-uniform when the ultimate horizontal bearing capacity is reached, and the radial earth pressure decreases with the increase of the angle θ. The calculation results by using Eq.(3) are in good agreement with the measured results, which indicates that the radial earth pressure on the passive side in the limit state is non-uniformly distributed and can be characterized by Eq.(3).

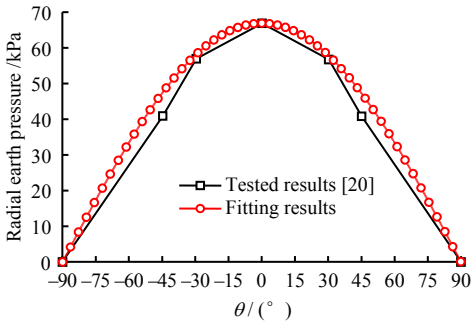

Fig. 3 Comparison of calculation results of radial earth pressure on passive side

Yang et al. [23] simulated four conditions with the pile rotation angle θ' of 0°, 0.5°, 1.0° and 2.0° and provided the lateral component distribution of radial earth pressure at depths of z/d = 1.0 and z/d = 5.5 (d for the pile diameter). At z/d = 1.0, the position of this depth is above the rotation point, and the passive side

ranges from $(-90^{o},0^{o})$ to $(0^{o},90^{o})$; at z/d = 5.5, the position of this depth is below the rotation point, with the passive side range of $(-180^{o},-90^{o})$ and $(90^{o},180^{o})$. The radial earth pressure distribution on the passive side does not change at different depths, and those at the same depth and different rotation angles are also the same. When the rotation angle reaches 2.0° (at which point the pile deformation is large enough), the lateral bearing capacity can be considered to have reached the limit value. Taking the depth of z/d = 1.0 as an example, based on the maximum radial earth pressure (radial earth pressure at $\theta = 0°$), the horizontal components of radial earth pressure on the passive side at different rotation angles were calculated by using Eq. (3) and then were compared with the simulation results, as shown in Fig. 4. Eq. (3) can accurately predict the horizontal components of the radial earth pressure on the passive side during the entire process of the lateral bearing capacity from 0 to the limit value, which indicates the rationality of Eq. (3).

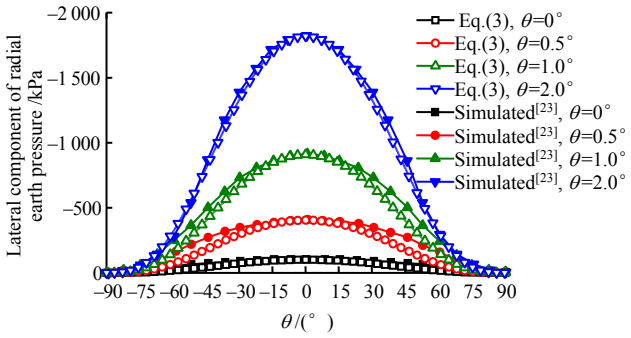

Fig. 4 Comparison of calculation results of horizontal component of radial earth pressure on passive side

The compression on the passive side soil increases with the increase of lateral displacement, so how to establish a computational model of the variation of radial earth pressure on the passive side with the lateral displacement is the key to solving the shaft resisting moment and the variation of pile axial force. Two approaches have been found from the existing literature: one is to establish the relationship between the radial earth pressure at each point on the passive side $\sigma_{pr,i}$ and the lateral displacement, and then to solve the pile axial force variation and the shaft resisting moment at each point; the other is to establish the relationship between the maximum radial earth pressure $\sigma_{pr,max}$ and the lateral displacement on the passive side, and then to solve the pile axial force variation and the shaft resisting moment based on the relation between $\sigma_{pr,max}$ and $\sigma_{pr,i}$. Obviously, method 1 is too complicated while method 2 is easy to be implemented. At present, there are few theoretical studies on the relationship between the maximum radial earth pressure on the passive side $\sigma_{pr,max}$ and the lateral displacement. Li et al.[19] assumed that the maximum radial earth pressure on the passive side $\sigma_{pr,max}$ is the ratio of the total soil resistance to the pile diameter, which in essence is the assumption that the radial earth pressure on the passive side is uniformly distributed. Song et al.[24] adopted the Rankine's earth pressure model considering deformation proposed by Mei et al.[25] to characterize the variation of the maximum radial earth pressure on the passive side $\sigma_{pr,max}$ with the lateral displacement, i.e. $\sigma_{pr,max} = \gamma z K(y)$ ($K(y)$ is the coefficient of earth pressure); however, the passive ultimate earth pressure was assumed as $\sigma_{pr,u} = K_p \gamma z$ (i.e. $K(y) = K_p$), which is much smaller than the ultimate earth pressure on the passive side obtained from the centrifugal test by Zhang et al.[26]. Based on these previous studies, it has been assumed that the soil on the active side is detached from the pile and that the radial earth pressure exists only on the passive side. The lateral component of the radial earth pressure was solved according to Eq.(3) and integrated to obtain the total soil resistance p as

$$p = 2\int_0^{\pi/2} \frac{d}{2}\sigma_{pr,i}\cos\theta \mathrm{d}\theta = \frac{\pi d}{4}\sigma_{pr,max} \tag{4}$$

The relation between the maximum radial earth pressure on the passive side and the total soil resistance can be obtained according to Eq. (4) as

$$\sigma_{pr,max} = \frac{4p}{\pi d} \tag{5}$$

Equation 5 shows the relation between the maximum radial earth pressure on the passive side and the lateral displacement since soil resistance is a function of lateral displacement. To verify the accuracy of Eq.(5), the maximum radial earth pressure on the passive side that changes with the lateral displacement was calculated by using Eq.(5)and other two methods proposed by Mei et al. [25] and Li et al. [19], according to the pile–soil parameters in literature[20], with the results shown in Fig. 5.

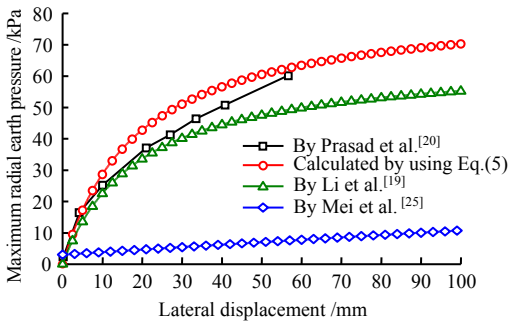

Fig. 5 Calculation results of the maximum radial earth pressure on passive side

As shown in Fig. 5, the maximum radial earth pressure calculated using the method proposed by Mei et al.[25] is much smaller than the measured one, that calculated using the method of Li et al.[19] is smaller, while the maximum radial earth pressure obtained by using Eq.(5) is in the best agreement with the measured results, which indicates that Eq.(5) can well

characterize the relation between the maximum radial earth pressure on the passive side and the lateral displacement.

The pile axial force variation and the shaft resisting moment can be easily solved according to Eqs.(3) and (5). The distribution of vertical frictional resistance on the passive side is shown in Fig.(6). In Fig. 6 (a), the vertical frictional resistance on the passive side decreases gradually from $\theta = 0°$ to $\theta = \pm 90°$. The vertical frictional resistance τ_{i} at any depth per unit pile length at the angle θ was calculated using the product of the radial earth pressure on the passive side and the frictional coefficient :

$$\tau_{\mathrm{i}} = \mu\sigma_{\mathrm{pr,i}} \tag{6}$$

where μ is the vertical frictional coefficient at the pile–soil interface. The one for sand foundation is calculated by the following equation:

$$\mu = \tan\delta \tag{7}$$

where δ is the friction angle at the pile–soil interface. Tomlinson et al. [27] suggested $\delta = (0.5–0.7)\varphi'$ for smooth piles and $\delta = (0.7–0.9)\varphi'$ for rough piles, φ' is the effective internal friction angle.

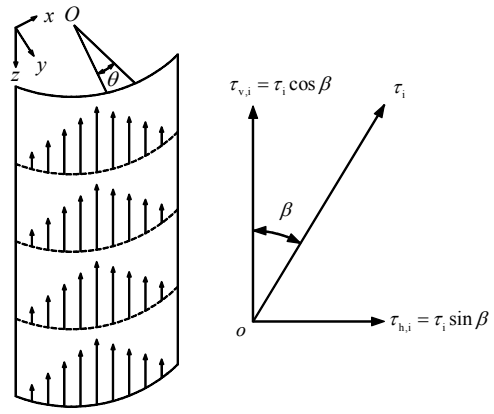

(a) Vertical frictional resistance (b) Computational model

Fig. 6 Distribution of vertical frictional resistance, and computational model

The vertical frictional resistance on the passive side is not along the vertical direction, but at an angle β to it, as shown in Fig. 6(b). Most existing calculation methods focus on small deformation conditions, assuming that the vertical frictional resistance on the passive side is along the vertical direction and ignoring the effect of pile rotation angle. However, under large deformation conditions, the effect of pile rotation angle should be considered, otherwise the variation of pile axial force caused by the frictional resistance on the passive side will be overestimated. With the pile rotation angle considered, the variation of pile axial force f per unit pile length at any depth z caused by the frictional resistance is obtained as below:

$$f = 2\int_0^{\pi/2}\tau_{\mathrm{v},i}\mathrm{d}\theta = 2\int_0^{\pi/2}\tau_i\cos\beta\mathrm{d}\theta = \frac{4\mu p}{\pi}\cos\beta \tag{8}$$

where $\beta = \dfrac{\mathrm{d}y}{\mathrm{d}z}$.

The shaft resisting moment is independent of the pile rotation angle, and the calculation model is shown in Fig.7. An infinitesimal arc in the cross-section at depth z is taken for analysis, the distance x_i from the center point of the i-th infinitesimal arc to the axis AC is

$$x_i = \frac{d}{2}\cos\theta \tag{9}$$

The shaft resisting moment $\mathrm{d}M_{\mathrm{s}}$ generated by the i-th arc to the AC axis of the unit length is

$$\mathrm{d}M_{\mathrm{s}} = \frac{d}{2}x_i\tau_{\mathrm{i}}\mathrm{d}\theta \tag{10}$$

By integrating, the total shaft resisting moment M_{s} generated by the vertical frictional resistance of arcs AB and BC on the AC axis of the pile section of the unit length is

$$M_{\mathrm{s}} = 2\int_0^{\pi/2}\frac{d}{2}x_i\tau_{\mathrm{i}}\mathrm{d}\theta = \frac{\mu dp}{2} \tag{11}$$

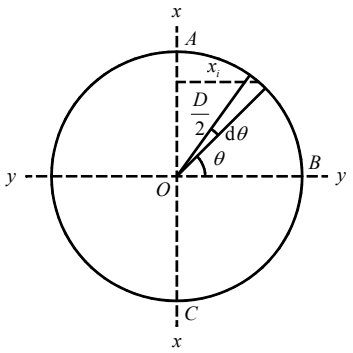

Fig. 7 Computational model for shaft resisting moment

2.4 Deflection differential equation

A pile element with a length of $\mathrm{d}z$ is chosen at any depth z. The upper section of the element is subjected to the bending moment M, the shear force Q and the axial force P; the lower section is subjected to the bending moment $M + \mathrm{d}M$, the shear force $Q + \mathrm{d}Q$ and the axial force $P + \mathrm{d}P$; the passive side is subjected to the soil resistance p, the vertical frictional resistance f, and the total shaft resisting moment M_{s}, as shown in Fig. 8.

It can be obtained from the moment equilibrium condition as

$$M + \mathrm{d}M - M - Q\mathrm{d}z - P\mathrm{d}y + p\frac{(\mathrm{d}z)^2}{2} + M_{\mathrm{s}}\mathrm{d}z = 0 \tag{12}$$

By neglecting the second-order term and dividing both sides simultaneously by $\mathrm{d}z$, Eq.(12) can be simplified to

$$\frac{\mathrm{d}M}{\mathrm{d}z} - Q - P\frac{\mathrm{d}y}{\mathrm{d}z} + M_{\mathrm{s}} = 0 \tag{13}$$

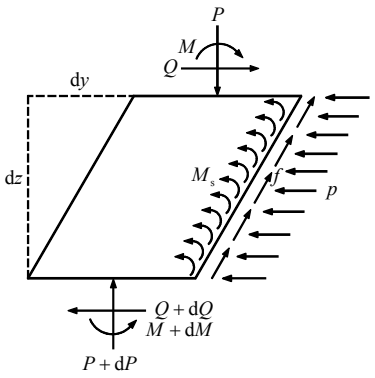

Fig. 8 Forces on pile element

The axial force P at any depth z is

$$P = V + A_p\gamma_p z - \int_0^z \frac{4\mu p\cos\beta}{\pi}\mathrm{d}z \tag{14}$$

where A_p is the section area; γ_p is the unit weight of the pile.

By finding the first-order derivative of Eq. (13) with respect to depth z and substituting $E_pI_p\dfrac{\mathrm{d}^2y}{\mathrm{d}z^2} = -M$ (E_p is the elastic model, I_p is the moment of inertia of the pile cross-section), $\dfrac{\mathrm{d}Q}{\mathrm{d}z} = p$, $\dfrac{\mathrm{d}P}{\mathrm{d}z} = A_p\gamma_p - \dfrac{4\mu p\cos\beta}{\pi}$, we have

$$E_pI_p\frac{\mathrm{d}^4y}{\mathrm{d}z^4} - \left(V + A_p\gamma_p z - \int_0^z \frac{4\mu p\cos\beta}{\pi}\mathrm{d}z\right)\frac{\mathrm{d}^2y}{\mathrm{d}z^2} - \left(A_p\gamma_p - \frac{4\mu p\cos\beta}{\pi}\right)\frac{\mathrm{d}y}{\mathrm{d}z} + \frac{\mu d}{2}\frac{\mathrm{d}p}{\mathrm{d}z} + p = 0 \tag{15}$$

Equation 15 is the derived deflection differential equation of flexible single pile under $V\rightarrow H$ loading path. It is a high-order differential equation with variable coefficients and also contains integral of composite function. It cannot be solved directly to obtain a reasonable analytical solution, and therefore, Eq.(15) with the given boundary condition is numerically solved in MATLAB. For flexible long piles, the bending moment and shear force at the pile end are both 0 while the pile top is free at ground surface and subjected to the lateral load H_0 and the bending moment M_0, so the boundary conditions are

$$\left.\begin{aligned} E_pI_p\cdot(y'')_{z=0} &= M_0 \\ E_pI_p\cdot(y''')_{z=0} &= H_0 \\ E_pI_p\cdot(y'')_{z=L} &= 0 \\ E_pI_p\cdot(y''')_{z=L} &= 0 \end{aligned}\right\} \tag{16}$$

which are used to calculate the pile deformation and the internal force at the depth of the corresponding step length.

3 Verification

3.1 Example 1

Lesny et al. [28] simulated large-diameter steel-pipe pile under lateral loading, with a pile diameter of 6.0 m, a pile length of 38.9 m and a pile top bending moment of 855 MN • m. Foundation soil was sand with an internal friction angle of 40.5°, a unit weight of 17 kN/m^3 and a relative density of 0.55. According to literature [16], $n_{h,max} = 35$ MN/m^3. Method 1: the maximum radial earth pressure is $\sigma_{pr,max} = p/d$. Method 2: the maximum radial earth pressure is $\sigma_{pr,max} = \gamma zK(y)$. Method 3: without considering the friction effect. The lateral displacements of pile shaft calculated using the proposed method, Method 1, Method 2, and Method 3 separately were compared with the simulation results, as shown in Fig.9. The lateral displacements of the pile top calculated are shown in Table 1. Learnt from Fig. 9 and Table 1, the lateral displacement will be overestimated without considering the friction effect; it will be slightly reduced when the maximum radial earth pressure on the passive side is assumed to be $\sigma_{pr,max} = \gamma zK(y)$, and will be further reduced when the maximum radial earth pressure on the passive side is assumed to be $\sigma_{pr,max} = p/d$; however, the calculated lateral displacement is closest to the simulation result when adopting the proposed method, which verifies the accuracy of the proposed method.

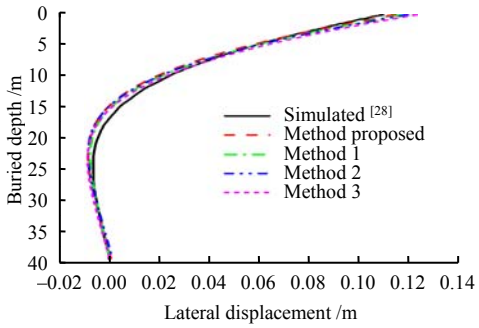

Fig. 9 Comparison of calculated lateral displacements of pile shaft with different methods

Table 1 Comparison of lateral displacements of pile top with different methods

Method	Simulated result[28]	Method proposed	Method 1	Method 2	Method 3
Lateral displacement of pile top /mm	109.67	114.29	117.06	119.08	122.69

The vertical frictional resistance, the shaft resisting moment and the axial force calculated are further presented in Fig.10. Figs.10(a) and 10(b) show that the vertical frictional resistance and the shaft resisting moment are distributed in an inverse S-shape along the depth. The critical point is located approximately 15 m below ground level, corresponding to the first point with zero displacement (Fig.9). In addition, the vertical frictional resistance and the shaft resisting moment were underestimated by both of method 1 and method 2, resulting in large predicted lateral displacements.

As shown in Fig. 10(c), the pile axial force caused by the vertical frictional resistance on the passive side tends to increase, then decrease and then increase in the opposite direction along the depth. The depth of the critical point is approximately 25 m, corresponding to place where the maximum negative vertical frictional resistance is (Fig.10(a)). Furthermore, the pile axial force caused by the vertical frictional resistance, which is beneficial for the lateral deformation, will be underestimated by both of method 1 and method 2, thus leading to overestimating the lateral deformation. Therefore, the methods derived for calculating the vertical frictional force, the axial force, and the shaft resisting moment can more accurately consider the benefit of friction effect and thus more accurately predict the pile lateral response.

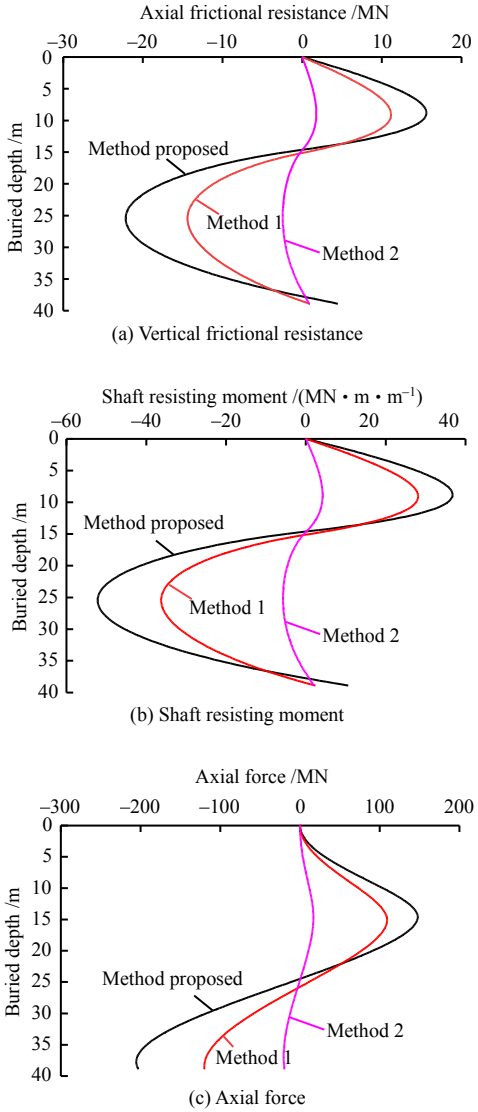

Fig. 10 Comparison of calculation results with different methods

3.2 Example 2

Farhan et al. [12] studied the effect of pre-applied vertical forces on the lateral bearing capacity by means of model tests. The model pile was a close-ended steel pipe with an external diameter of 0.03 m and a wall thickness of 2 mm, buried 0.75 m deep, with a vertical ultimate bearing capacity of 1 417 N. Most of the model pile was in the upper medium dense sand and only the bottom was embedded in the lower dense sand. The lateral bearing capacity mainly depends on the strength of the upper soil, so the parameters of the upper medium dense sand were adopted to simplify the calculation, with the unit weight of 16.01 kN/m^3, the angle of internal friction of 34°, and the relative density of 0.55. The test results under three conditions of 0, 0.4V_{ult} and 0.8V_{ult} were selected for comparison.

Figure 11 shows the calculated and tested lateral bearing capacities under different vertical forces. As can be seen from Fig.11(a), the lateral bearing capacity calculated theoretically agrees well with the measured one at the same lateral displacement when the vertical force is 0. From Figs. 11(b) and 11(c), the calculated lateral bearing capacity is much smaller than the measured one without considering the enhancement of the ultimate soil resistance by the pre-applied vertical force, and the two are in good agreement when considering the enhancement of the soil resistance, which verifies the correctness of the method proposed.

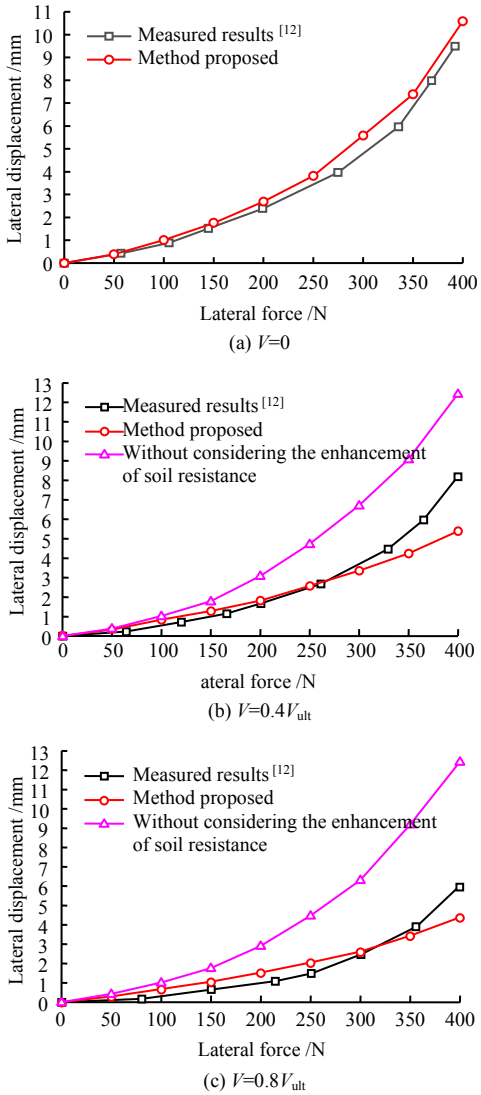

Fig. 11 Comparison of calculated lateral bearing capacities of pile under different vertical loads

4 Effect of pre-applied vertical force on lateral bearing capacity of flexible single pile

The parameters in Example 2 were selected to analyze the effect of different pre-applied vertical forces on the lateral bearing capacity under the same lateral force. The lateral force at the pile top is 400 N, and the pre-applied vertical forces are 0, $0.4V_{ult}$ and $0.8V_{ult}$.

The calculated lateral displacements under different pre-applied vertical forces are shown in Fig. 12(a). The lateral displacements decreases by 49% and 59%, respectively, when the pre-applied vertical force increases from 0 to $0.4V_{ult}$ and $0.8V_{ult}$, which indicates that the pre-applied vertical force will reduce the lateral displacement while enhance the lateral bearing capacity under the same lateral force. But the enhancement gradually decreases as the pre-applied vertical force increases. The calculated pile rotation angles under different pre-applied vertical forces are shown in Fig.12(b). The rotation angle decreases non-linearly along the depth, with the rate of decrease first increasing and then decreasing. When the pre-applied vertical force increases from 0 to $0.4V_{ult}$ and $0.8V_{ult}$, the rotation angle decreases by 37% and 46%, respectively.

The calculated bending moment under different pre-applied vertical forces are shown in Fig. 12(c). The bending moment tends to increase first and then decrease along the depth. The maximum bending moment decreases with the increase of the pre-applied vertical force and its position moves upwards. When the pre-applied vertical force increases from 0 to $0.4V_{ult}$ and $0.8V_{ult}$, the maximum bending moment decreases by 25% and 32%, respectively, and its corresponding depth decreases by 23% and 29%, respectively. Two reasons can be explained for this. Firstly, the increase in bending moment caused by the $P-\Delta$ effect generated by the pre-applied vertical force is not as strong as the increase in shaft resisting moment caused by the increases in lateral soil resistance and shaft resisting moment. Secondly, the decrease in lateral displacement leads to the decrease in bending moment caused by the lateral force at the pile top.

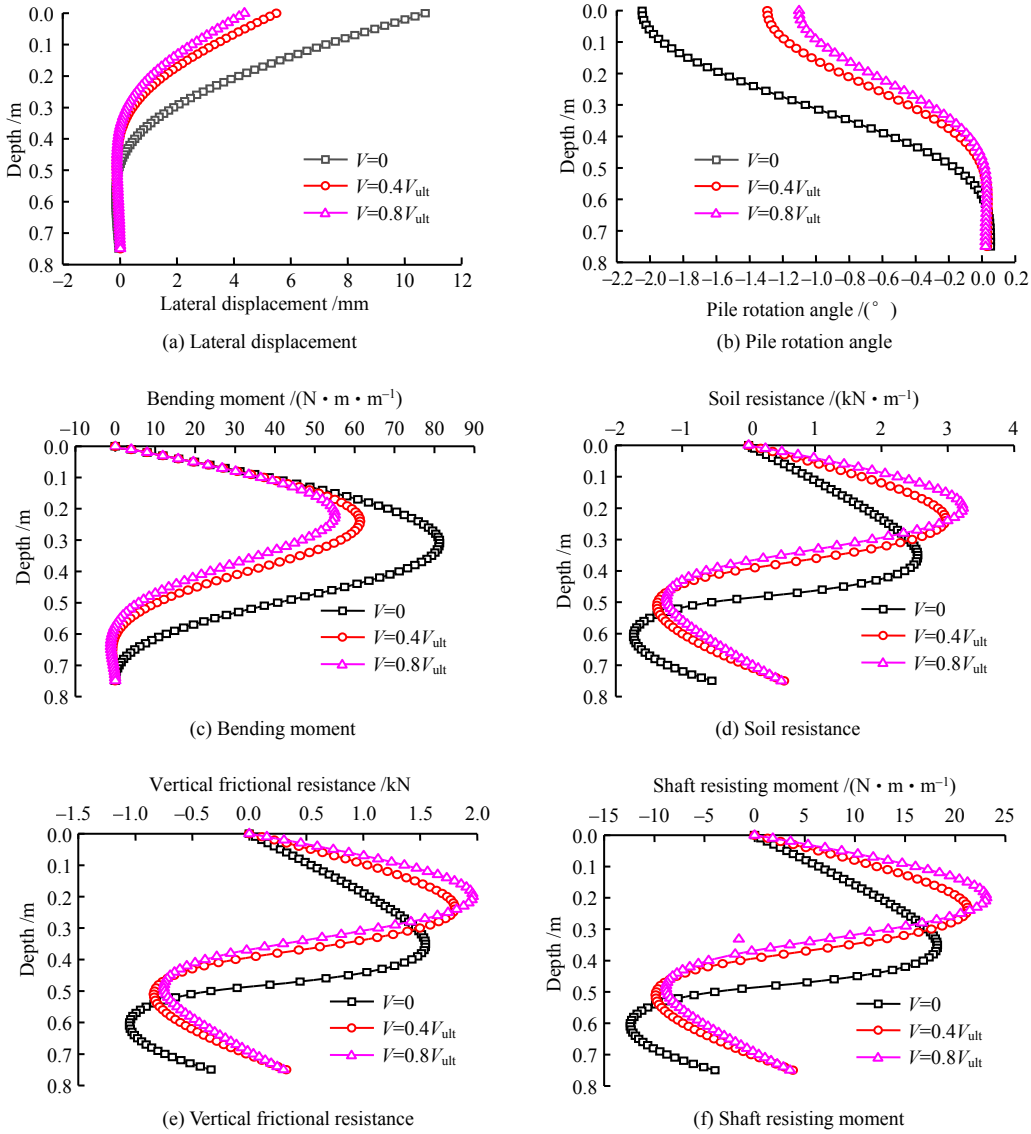

(a) Lateral displacement (b) Pile rotation angle

(c) Bending moment (d) Soil resistance

(e) Vertical frictional resistance (f) Shaft resisting moment

Fig. 12 Comparison of calculation results under different vertical loads

The calculated lateral soil resistance under different pre-applied vertical forces is shown in Fig. 12(d). The lateral soil resistance is distributed in an inverse S-shape along the depth, and the maximum absolute value of negative soil resistance is less than the maximum of positive soil resistance. The inflection point moves up as the pre-applied vertical force increases. The soil resistance above the inflection point increases and that below the inflection point decreases. When the pre-applied vertical force increases from 0 to $0.4V_{\text{ult}}$ and $0.8V_{\text{ult}}$, the maximum positive soil resistance increases by 14% and 27%, respectively, and the corresponding depth decreases by 33% and 43%, respectively; the maximum absolute value of negative soil resistance decreases by 20% and 29%, respectively, and the corresponding depth decreases by 16% and 20%, respectively. The reason for this is that the lateral displacement mainly occurs in the shallow soil, and the increase of the pre-applied vertical force leads to the ultimate lateral soil resistance to increase. As a result, the lateral soil resistance increases significantly; for the soil around the pile below the first point with zero displacement, the ultimate soil resistance increases, but the lateral displacement decreases, so the soil resistance decreases.

It can be seen from Eqs. (8) and (11) that the trends of vertical frictional resistance and shaft resisting moment are the same as that of the soil resistance, with only numerical differences. The vertical frictional resistance and shaft resisting moment calculated under different pre-applied vertical forces are shown in Figs.12(e) and 12(f), respectively. As the pre-applied vertical force increases, the inflection point moves up, the vertical frictional resistance and shaft resisting moment above the inflection point increase and those below the inflection point decrease.

5 Conclusions

Considering the effect of pre-applied vertical forces on the lateral bearing capacity of single pile and the mechanical parameters of the soil around the pile, the numerical solution for the lateral bearing capacity of flexible single pile has been derived with accounting for the modified *p*–*y* curve, the axial force variation caused by the pile dead weight and the frictional resistance on the passive side, the $P-\Delta$ effect, and the shaft resisting moment, with conclusions below:

(1) The distribution of the radial earth pressure on the passive side can be accurately characterized by using the cosine function, based on which the equation of the maximum radial earth pressure on the passive side and the total soil resistance derived can precisely describe the variation of the maximum radial earth pressure with the lateral displacement, whereas the maximum radial earth pressure on the passive side is underestimated using either of $\sigma_{\text{pr,max}} = \gamma z K(y)$ or $\sigma_{\text{pr,max}} = p / d$.

(2) The derived analytical expression for the variation of pile axial force can more accurately characterize the effect of the frictional resistance on the passive side on the pile axial force as the effect of the rotation angle β has been considered and can be used for large deformation conditions.

(3) The pre-applied vertical force increases the soil resistance, vertical frictional resistance, and shaft resisting moment in the shallow soil and reduces the lateral displacement, rotation angle and bending moment of the pile. With the increase of the pre-applied vertical force, its enhancement on the lateral bearing capacity of the flexible single pile gradually decreases.

(4) The modified empirical formula for ultimate soil resistance recorded in literature [14] has been adopted in the proposed method of analyzing the lateral bearing capacity of flexible single pile under the $V \rightarrow H$ loading path, and it is only applicable to sand foundations and has yet to be further studied for different foundation conditions.

References

[1] HUANG Fu-yun, ZHOU Zhi-ming, ZHUANG Yi-zhou, et al. Experiment on interaction of high performance concrete pile-soil in IAJBs[J]. Rock and Soil Mechanics, 2022, 43(3): 591–601.

[2] FENG Zhong-ju, MENG Ying-ying, ZHANG Cong, et al. Dynamic response and *p*-*y* curve of pile groups in liquefaction site under strong earthquake[J]. Rock and Soil Mechanics, 2022, 43(5): 1289–1298.

[3] ZHU Yan-peng, WU Lin-ping, SHI Duo-bang, et al. Application of nonlinear soil resistance-pile lateral displacement curve based on Pasternak foundation model in foundation pit retaining piles[J]. Rock and Soil Mechanics, 2022, 43(9): 2581–2591.

[4] AI Zhi-yong, GU Gan-lin, LI Pan-cong, et al. Analysis of interaction between fractional viscoelastic saturated soils and laterally loaded pile groups[J]. Rock and Soil Mechanics, 2022, 43(11): 2933–2940.

[5] KARTHIGEYAN S, RAMAKRISHNA V V G S T, RAJAGOPAL K. Influence of vertical load on the lateral response of piles in sand[J]. Computers and Geotechnics, 2006, 33(2): 121–131.

[6] ANAGNOSTOPOULOS C, GEORGIADIS M. Interaction of axial and lateral pile responses[J]. Journal of Geotechnical Engineering, 1993, 119(4): 793–798.

[7] ABBAS J M, HUSSAIN Q I. The effect of pile cross section on the lateral behavior of piles under combined loading[J]. Journal of Engineering Science and Technology Review, 2018, 11(3): 174–179.

[8] LU W J, ZHANG G. Influence mechanism of vertical-horizontal combined loads on the response of a single pile in sand[J]. Soils and Foundations, 2018, 58(5): 1228–1239.

[9] ZHAO Chun-feng, WANG Wei-zhong, ZHAO Cheng, et al. lateral bearing capacity of single piles under vertical and moment load in sand[J]. Chinese Journal of Rock

Mechanics and Engineering, 2013, 32(1): 184–190.

[10] ZOU Xin-jun LU Peng-kun. Contrastive analysis on effect of vertical force on horizontal bearing capacity of a single pile in medium sand and soft clay[J]. Journal of Hunan University (Natural Sciences), 2018, 45(11): 110–119.

[11] KARTHIGEYAN S, RAMAKRISHNA V V G S T, RAJAGOPAL K. Numerical investigation of the effect of vertical load on the lateral response of piles[J]. Journal of Geotechnical and Geoenvironmental Engineering, 2007, 133(5): 512–521.

[12] FARHAN I S, SHAKIR A M, IBRAHIM A A F. Performance of a single pile combined axial and lateral loads in layered sandy soil[J]. Journal of Engineering and Sustainable Development, 2018, 22(1): 121–36.

[13] MU L L, KANG X Y, FENG K, et al. Influence of vertical loads on lateral behaviour of monopiles in sand[J]. European Journal of Environmental and Civil Engineering, 2018, 22(Supp1.): 286–301.

[14] CHATTERJEE K, CHOUDHURY D. Analytical and numerical approaches to compute the influence of vertical load on lateral response of single pile[C]//The 15th Asian Regional Conference on Soil Mechanics and Geotechnical Engineering (15ARC)-New Innovations and Sustainability. Fukuoka: [s. n.], 2015: 1319–1322.

[15] O'NEILL M W, MURCHINSON J M. An evaluation of *p-y* relationships in sand[R]. Washington D C: American Petroleum Institute, 1983.

[16] ZHANG L Y. Nonlinear analysis of laterally loaded rigid piles in cohesionless soil[J]. Computers and Geotechnics, 2009, 36(5): 718–724.

[17] ZHU Bin, ZHU Rui-yan, LUO Jun, et al. Model tests on characteristics of ocean and offshore elevated piles with large lateral deflection[J]. Chinese Journal of Geotechnical Engineering, 2010, 32(4): 521–530.

[18] ZHANG Xiao-ling, ZHAO Jing-jiu, SUN Yi-long, et al. An analysis method for the horizontal bearing capacity of pile foundation based on the cavity expansion theory[J]. Engineering Mechanics, 2021, 38(2): 232–241, 256.

[19] LI Hong-jiang, LIU Song-yu, TONG Li-yuan, et al. Method to analyze lateral bearing capacity of small deformation piles considering friction effect[J]. Chinese Journal of Rock Mechanics and Engineering, 2018, 37(1): 230–238.

[20] PRASAD Y V S N, CHARI T R. Lateral capacity of model rigid piles in cohesionless soils[J]. Soils and Foundations, 1999, 39(2): 21–9.

[21] LIN H, NI L, SULEIMAN M T, et al. Interaction between laterally loaded pile and surrounding soil[J]. Journal of Geotechnical and Geoenvironmental Engineering, 2015, 141(4): 1–11.

[22] HUANG Shen, ZHAI En-di, XU Cheng-shun, et al. A method of analyzing laterally loaded monopiles considering the influence of additional resistance[J]. Engineering Mechanics, 2022, 39(6): 156–168.

[23] YANG M, GE B, LI W C. Force on the laterally loaded monopile in sandy soil[J]. European Journal of Environmental and Civil Engineering, 2020, 24(10): 1–20.

[24] SONG Lin-hui, MEI Guo-xiong, ZAI Jin-min. Application of soil pressure model considering displacements to lateral loaded piles[J]. Rock and Soil Mechanics, 2007, 28(5): 1035–1039.

[25] MEI Guo-xiong, ZAI Jin-min. Earth pressure calculating method considering displacement[J]. Rock and Soil Mechanics, 2001, 22(4): 83–85.

[26] ZHANG L Y, SILVA F, GRISMALA R. Ultimate lateral resistance to piles in cohesionless soils[J]. Journal of Geotechnical and Geoenvironmental Engineering, 2005, 131(1): 78–83.

[27] TOMLINSON M, WOODWARD J. Pile design and construction practice[M]. New York: Taylor & Francis, 2007: 172–173.

[28] LESNY K, WIEMANN J. Finite-element-modelling of large diameter monopiles for offshore wind energy converters[C]//GeoCongress. Atlanta: [s. n.], 2006: 1–6.